

Cite this: *Chem. Sci.*, 2024, 15, 17944

All publication charges for this article have been paid for by the Royal Society of Chemistry

Received 10th September 2024

Accepted 2nd October 2024

DOI: 10.1039/d4sc06144f

rsc.li/chemical-science

# Structure-constraint induced increase in Lewis acidity of tris(*ortho*-carboranyl)borane and selective complexation with Bestmann ylides†

Libo Xiang,<sup>ab</sup> Junyi Wang,<sup>c</sup> Alexander Matler<sup>ab</sup> and Qing Ye<sup>ab</sup>

The Lewis acidity of tris(*ortho*-carboranyl)borane has been slightly increased by mimicking the structural evolution from triarylborane to 9-aryl-9-borafluorene. The *o*-carborane-based analogue ( $C_2B_{10}H_{10}$ )<sub>2</sub>B( $C_2B_{10}H_{11}$ ), obtained *via* salt elimination between  $LiC_2B_{10}H_{11}$  and  $(C_2B_{10}H_{10})_2BBr$ , has been fully characterized. Gutmann–Beckett and computational fluoride/hydride ion affinity (FIA/HIA) studies have confirmed the increase in Lewis acidity, which is attributable to structural constraint imposed by the CC-coupling between two carboranyl groups. Selective complexation of  $(C_2B_{10}H_{10})_2B(C_2B_{10}H_{11})$  with Bestmann ylides  $R_3PCCO$  ( $R = Ph, Cy$ ) has been achieved, enabling further conversion into the zwitterionic phospholium salt through NHC-catalyzed proton transfer.

Triarylboranes feature a three-coordinate six-electron boron center. They constitute a highly significant class of Lewis acids. Over the past century, the continuous focus on triarylborane chemistry has led to its substantial development.<sup>1</sup> This has resulted in a wide array of applications across diverse fields, such as sensory materials,<sup>2</sup> optoelectronic materials,<sup>3</sup> small molecule activation,<sup>4</sup> and catalysis.<sup>5</sup> A significant benefit derived from the triarylborane motif is the feasibility of tuning the steric hindrance and electronic properties of the boron center by introducing appropriate substituents on the aryl groups.

Remarkably, the coupling of one *ortho*-carbon atom from each of the two aryl groups in triarylborane results in the creation of another significant class of molecules known as 9-borafluorenes.<sup>6</sup> In these molecules, the boron atom is positioned within an anti-aromatic borole unit,<sup>7</sup> giving rise to distinctive properties,<sup>8</sup> including an increase of the Lewis acidity. For instance, triphenylborane (Fig. 1. **A**) demonstrates a fluoride ion affinity (FIA) of  $354.35 \text{ kJ mol}^{-1}$  (Table S2†), while the FIA of 9-phenyl-9-borafluorene (**B**) is elevated to  $366.27 \text{ kJ mol}^{-1}$  (Table S2†).<sup>9</sup> Moreover, despite the removal of two *ortho*-electron-withdrawing fluorine atoms, the FIA of **D**

( $456.67 \text{ kJ mol}^{-1}$ , Table S2†) is still higher than that of **C** ( $452.68 \text{ kJ mol}^{-1}$ , Table S2†).<sup>9</sup>

On the other hand, three-dimensional (3D) aromatic *ortho*-dicarbadodecaborane (*o*-carborane) can be regarded as a 3D analogue of benzene, and there has been a growing interest in carborane-based 3D analogues of conventional aryl-substituted boron compounds in recent years.<sup>10</sup> In fact, the carboranyl substituted boron compounds have displayed numerous properties worthy of further exploration and development, including Lewis superacidity,<sup>11</sup> fluorescence,<sup>11,12</sup> the capability of small molecule activation,<sup>13</sup> and unique boron radical electronic structures.<sup>14</sup> The successful synthesis of the three-dimensional analogue of **A**, *i.e.* **E** as a Lewis superacid (LSA) stands as

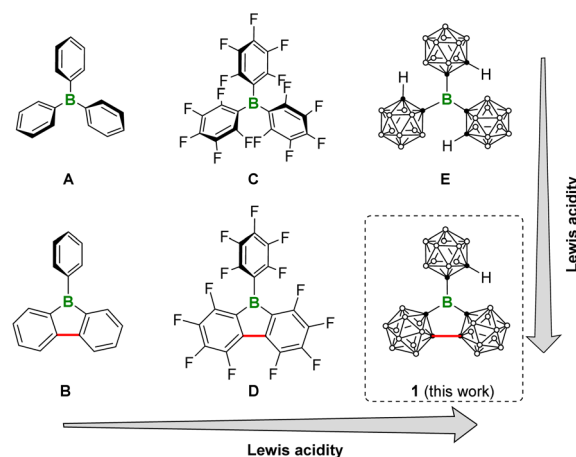


Fig. 1 The trend in Lewis acidity among triarylboranes, 9-aryl-9-borafluorenes, and their respective carborane-based three-dimensional analogues.

<sup>a</sup>Institute for Inorganic Chemistry Julius-Maximilians-Universität Würzburg Am Hubland, 97074 Würzburg, Germany. E-mail: qing.ye@uni-wuerzburg.de

<sup>b</sup>Institute for Sustainable Chemistry & Catalysis with Boron Julius-Maximilians-Universität Würzburg Am Hubland, 97074 Würzburg, Germany

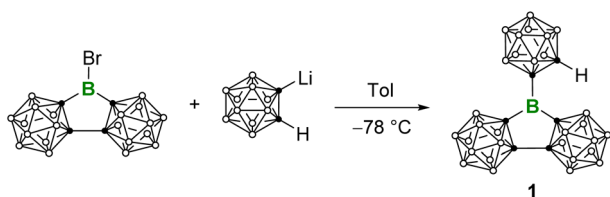
<sup>c</sup>Department of Chemistry, Southern University of Science and Technology, 518055 Shenzhen, P. R. China

† Electronic supplementary information (ESI) available: Experimental details, X-ray crystallographic and characterisation data. CCDC 2355581–2355583 and 2382930. For ESI and crystallographic data in CIF or other electronic format see DOI: <https://doi.org/10.1039/d4sc06144f>

a recent exemplary case.<sup>15</sup> In this context, curiosity arises as to whether a similar structural alteration of **E**, as illustrated in Fig. 1, could also enhance the Lewis acidity. Herein, we present the synthesis and Lewis acidity assessment of the carborane-based 3D analogue of **B**, *i.e.* **1**. Furthermore, it is believed that the ball-shaped carboranyl substituents create a sterically hindered spatial environment around the central boron atom. To validate this hypothesis, we examined its reaction with Bestmann ylide,<sup>16</sup> a Lewis base known for its ditopicity.

Compound **1** was attained by the reaction of  $\text{LiC}_2\text{B}_{10}\text{H}_{11}$  with an equimolar amount of  $(\text{C}_2\text{B}_{10}\text{H}_{10})_2\text{BBr}^{11d}$  at  $-78^\circ\text{C}$  (Scheme 1).  $^{11}\text{B}$  NMR spectrum displays a broad signal at  $\delta_{\text{B}}$  65, which is comparable to **E** ( $\delta_{\text{B}}$  67.2)<sup>15</sup> and falls in the range of three-coordinate boron centers. The C–H proton NMR signal at  $\delta_{\text{H}}$  3.70 is diagnostic while the corresponding C–H displays a singlet at  $\delta_{\text{C}}$  58.7 in the  $^{13}\text{C}\{\text{H}\}$  NMR spectrum. The atom connectivity was confirmed by single-crystal X-ray diffraction analysis (Fig. 2). Remarkably, the three  $\text{C}_{\text{carborane}}\text{–B}$  bonds (B–C1: 1.558(2) Å, B–C3/B–C6: 1.597(16) Å) are shorter than the  $\text{C}_{\text{carborane}}\text{–B}$  bonds (1.614(8)–1.627(7) Å) in  $\text{BoCb}_3$  (**E**).<sup>15</sup> In addition, the sum of angles around the central boron atom is  $359.8^\circ$ , indicating the trigonal-planar geometry. The C3–B–C6 angles of  $110.74(14)^\circ$  is close to the interior angle of a pentagon ( $108^\circ$ ). In addition, we exposed the  $\text{C}_6\text{D}_6$  solution of **1** to air and conducted hourly NMR monitoring, which revealed complete hydrolysis within 6 h.

The Gutmann–Beckett method<sup>17</sup> was applied to assess the Lewis acidity of **1**. With an LA/ $\text{Et}_3\text{PO}$  ratio of 1 : 1, the  $^{31}\text{P}$   $\Delta\delta$  of 34.9 for **1**/ $\text{Et}_3\text{PO}$  was slightly larger than that of **C**/ $\text{Et}_3\text{PO}$  ( $^{31}\text{P}$   $\Delta\delta$  33.9 in  $\text{C}_6\text{D}_6$ ). The acceptor number (AN) was 76.8 for **1** in  $\text{C}_6\text{D}_6$ , confirming its greater Lewis acidity than that of  $\text{B}(\text{C}_6\text{F}_5)_3$  (AN 65.6 in  $\text{C}_6\text{D}_6$ ) and **C** (AN 74.9 in  $\text{C}_6\text{D}_6$ ),<sup>15</sup> and comparable to that of the pyramidal borane: 9-boratriptycene (AN 76.2 in  $\text{CD}_2\text{Cl}_2$ ).<sup>18d</sup> It should be noted that the Gutmann–Beckett values are steric dependent. We calculated the buried volumes (%  $V_{\text{bur}}$ ) of **1** and **E** considering the steric bulk of the carboranyl substituents,<sup>19</sup> which indicate that both compounds have large %  $V_{\text{bur}}$  values (**1**: 67.7%, **E**: 73.3%, Table S5<sup>†</sup>). We also conducted calculations to further determine the FIA and hydride ion affinity (HIA) of **1** alongside **A**, to **E**, following the established literature protocols (Fig. 3).<sup>9</sup> The calculations indicate that **1** displays the highest FIA and HIA energies, clearly designating it as a Lewis superacid. Notably, **1** exhibits larger FIA and HIA values than **E**, which is consistent with the results obtained through the Gutmann–Beckett method. One possible primary reason why **1** is slightly more acidic than **E** should be due to the structural constraint through CC-coupling (marked in red in



Scheme 1 Synthesis of **1**.

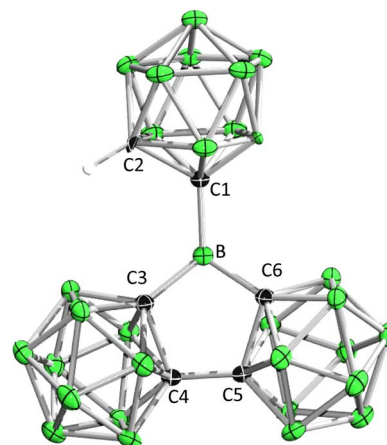


Fig. 2 Single crystal structure of complex **1** in the solid state. The hydrogen atoms were omitted for clarity. Thermal ellipsoids are drawn at the 50% probability level. Selected bond lengths [Å] and angles [°]: B–C1 1.558(2), B–C3 1.5966(16), B–C6 1.5966(16), C3–C4 1.6554(16), C4–C5 1.537(2), C5–C6 1.6554(16), C1–B–C3 124.55(7), C1–B–C6 124.55(7), C3–B–C6 110.74(14).

Fig. 1), which reduces the C3–B–C6 angle by *ca.*  $10^\circ$ , from  $120^\circ$  to *ca.*  $110^\circ$  compared to that in **E** (*ca.*  $120^\circ$ ). This deformation can be regarded as a ring-closure-enforced prepyramidalization, lowering the energy required for the structural deformation accompanying the complexation process.<sup>18</sup> Indeed, the calculated pyramidation energy of **1** ( $122.0\text{ kJ mol}^{-1}$ ) was lower than that of **E** ( $130.1\text{ kJ mol}^{-1}$ ). Overall, the results of FIA, HIA and Gutmann–Beckett method are all consistent, indicating the Lewis acidity order of **1** > **E** > **D** > **C** > **B** > **A**. Among these, **1** and **E** are the strongest acids in the sequence, further demonstrating that the inductive effect of *o*-carborane can effectively enhance the Lewis acidity of boranes. Additionally, the relatively lower pyramidation energy of **1** leads to its higher Lewis acidity compared to **E**.

Density functional theory (DFT) calculations were performed to provide further insight into the electronic properties of **1**, **E** and **D**. Compound **1** has appreciably lower LUMO and larger HOMO–LUMO gap (Fig. 4) than **D**, thus indicating the

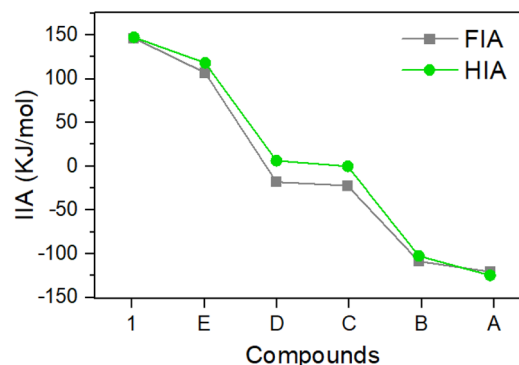


Fig. 3 Results of fluoride ion affinity (ref. to  $\text{SbF}_5$ ), hydride ion affinity (ref. to  $\text{B}(\text{C}_6\text{F}_5)_3$ ) analyses and Global Electrophilicity Index (GEI) of compound **1** and **A** to **E**.



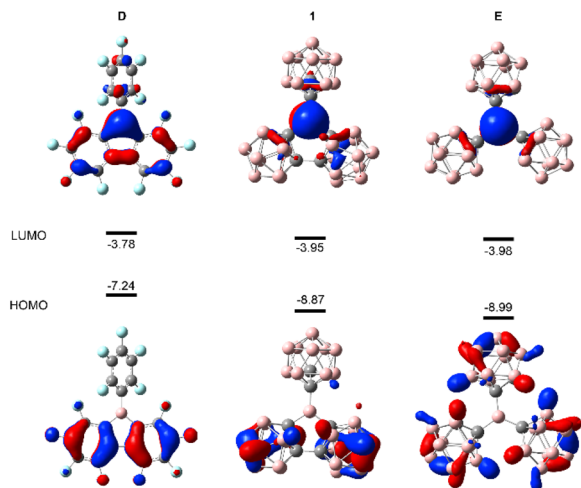
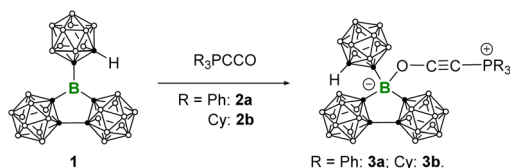


Fig. 4 Frontier orbitals of compound 1, D and E.

enhanced electron-accepting ability. This can be attributed to the strong electron-withdrawing effect of the carboranyl group. The LUMO of **E** is 0.03 eV lower in energy than that of **1**. Furthermore, Global Electrophilicity Index (GEI)<sup>18c,20,21</sup> was calculated for **1** and **A** to **E** (Table S4†). The GEI values of **1** (4.17), **E** (4.20) and **D** (4.40) are larger than those of **C** (3.78), **B** (2.59) and **A** (2.04). Notably, the GEI results do not correlate well with the GB-method and the FIA results, with **D** displaying a relatively higher GEI value.

With the Lewis superacidic borane **1** in hand, we decided to investigate its complexation reaction with Bestmann ylides. The prototype compound for Bestmann ylide is (triphenylphosphoranylidene)ketene  $\text{Ph}_3\text{PCCO}$ .<sup>22</sup> Several Bestmann ylide-supported transition metal complexes have been reported, where the ylidic carbon donates a pair of electrons to the transition metal center.<sup>23</sup> However, the reactivity of Bestmann ylides with three-coordinate boranes has been less explored. In fact, Bestmann ylides can undergo addition to  $\text{B}(\text{C}_6\text{F}_5)_3$ , either through the ylidic carbon or the carbonyl oxygen.<sup>24</sup> In contrast, because the central boron of **1** is surrounded by three spherical substituents, this could potentially enable a selective complexation reaction.

To this end, **1** was reacted with an equimolar amount of **2a** and **2b** in toluene, respectively (Scheme 2). The reactions were monitored by multinuclear NMR spectroscopy. In both cases, the three-coordinate boron  $^{11}\text{B}$  signal disappeared within 10 min, accompanied by the formation of a white precipitate. It is worth noting that the phosphonium  $^{31}\text{P}$  signal is merely slightly low-field shifted, in the case of **2a** from  $\delta_{\text{P}}$  3.1 to 5.2, **2b**



Scheme 2 Synthesis of **3**.

from  $\delta_{\text{P}}$  19.9 to 23.3, indicating that the electronic environment of the phosphorus center is not much affected upon complexation, and the oxygen-coordinated products **3a** and **3b** should be formed. Single crystal X-ray diffraction analysis unambiguously confirmed our hypothesis, showing that the terminal oxygen atom is bound to **1** (Fig. 5). While the bond lengths around boron increase from **1** (B–C1 1.558(2), B–C3 1.5966(16), B–C6 1.5966(16)) to **3** (**3a**: B–C3 1.683(2), B–C4 1.691(2), B–C1 1.653(2); **3b**: B–C3 1.691(4), B–C4 1.695(4), B–C1 1.664(4)), the sum of angles decreases from 359.8° in **1** to 339.5° in **3a** and 338.6° in **3b**, respectively, indicating a geometric change from trigonal planar to tetrahedral. In **3a**, the P–C2–C5–O unit features a nearly linear geometry, an elongated C5–O distance (1.264(19) vs. 1.195(2) Å) and a shortened C–C distance ((1.204(2) vs. 1.247(2) Å)), suggesting the oxyethynyl phosphonium type structure. The overall geometry of **3b** resembles that of **3a**. The infrared data for the  $\text{C}\equiv\text{C}$  stretching in compound **3** (**3a**: 2198  $\text{cm}^{-1}$ , **3b**: 2199  $\text{cm}^{-1}$ ) show a shift to higher wavenumbers than the uncoordinated Bestmann ylide (2090  $\text{cm}^{-1}$ ), indicating the strengthening of the carbon–carbon bond upon coordination. In addition, the notably shorter B–O distance in **3b** (1.522(4) Å) compared to the corresponding O-coordinated  $\text{B}(\text{C}_6\text{F}_5)_3\text{-2b}$  adducts (1.573(3) Å)<sup>24</sup> further confirms the higher Lewis acidity of **1** than  $\text{B}(\text{C}_6\text{F}_5)_3$ .

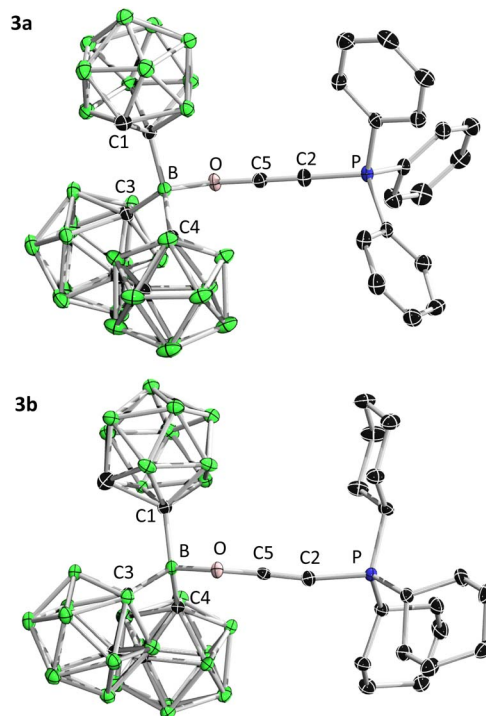
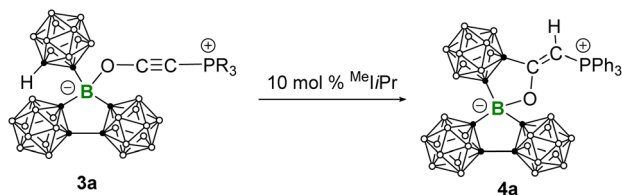


Fig. 5 Molecular structure of complex **3a** and **3b** in the solid state. The hydrogen atoms were omitted for clarity. Thermal ellipsoids are drawn at the 50% probability level. Selected bond lengths [Å] and angles [°]: **3a**, B–O 1.533(2), B–C1 1.653(2), B–C3 1.683(2), B–C4 1.691(2), O–C1 1.264(19), C1–C2 1.204(2), C2–P 1.701(17), O–C1–C2 174.19(17), C1–C2–P 179.96(17), C3–B–C4 104.18(12); **3b**, B–O 1.522(4), B–C1 1.664(4), B–C3 1.691(4), B–C4 1.695(4), O–C1 1.265(4), C1–C2 1.206(4), C2–P 1.713(3), O–C1–C2 172.60(3), C1–C2–P 166.5(3), C3–B–C4 104.1(2).





Scheme 3 Synthesis of 4a.

The zwitterionic phospholium salt **4a** was synthesized by treating **3a** with 10 mol% MeIiPr (1,3-diisopropyl-4,5-dimethylimidazole-2-ylidene) at room temperature (Scheme 3). The <sup>31</sup>P NMR spectrum showed the complete consumption of **3a** ( $\delta^{31}\text{P}$  5.17) within 10 min and the formation of a new species showing a downfield-shifted resonance at  $\delta^{31}\text{P}$  12.64. After workup, colorless single crystals of **4a** suitable for X-ray crystallography were obtained in a high yield (82%). X-ray analysis revealed a formal 1,2-addition of the CH of the exocyclic carborane cage to the alkynyl group of the coordinated Bestmann ylide, leading to a cyclization and the formation of **4a** featuring a planar C<sub>3</sub>BO five-membered heterocycle with an internal angle sum of 540.0° (Fig. 6). This reaction can also be evidenced by infrared spectroscopy, which indicated the disappearance of the characteristic C≡C stretching and a new C=C stretching at 1610 cm<sup>-1</sup> (Fig. S27 and S28†). A plausible mechanism for the formation of **4a** was proposed in Scheme 4. Following the deprotonation of **3a** by MeIiPr, the resulting *ortho*-carborane anion undergoes intramolecular nucleophilic attack on the alkynyl group, leading to cyclization into a carbene intermediate. Due to the generally higher Brønsted basicity of carbene than NHCs,<sup>25</sup> the carbene intermediate reclaims the proton from [MeIiPr-H]<sup>+</sup>, yielding the zwitterionic phospholium product **4a** and regenerating the free carbene for the next catalytic cycle. The strong Brønsted basicity of the carbene intermediate can also be reflected by the fact that all attempts using the common strong bases such as NaHMDS and NaH to deprotonate **4a** have failed: no reaction was observed.

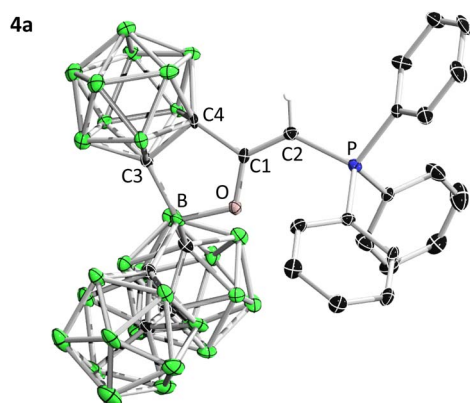
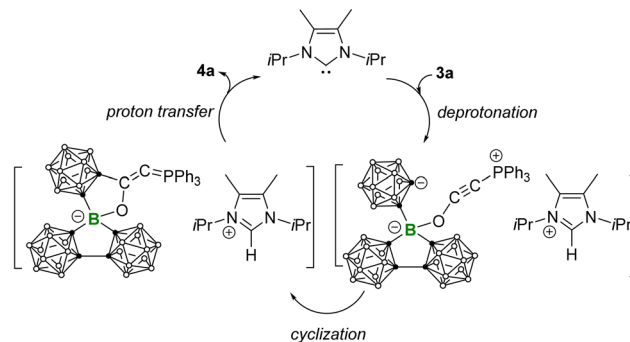


Fig. 6 Molecular structure of complex **4a** in the solid state. The hydrogen atoms were omitted for clarity. Thermal ellipsoids are drawn at the 50% probability level. Selected bond lengths [Å] and angles [°]: **4a**, B–O 1.5221(14), O–C1 1.3265(14), C1–C2 1.3469(17), C2–P 1.7633(14), C1–C2–P 130.04(10).



Scheme 4 Proposed reaction mechanism for the NHC-catalyzed proton transfer reaction.

In summary, drawing inspiration from the structural evolution from triarylboranes to 9-aryl-9-borafluorenes, we envisioned that the title compound **1** may exhibit even higher Lewis acidity than the Lewis superacidic tris(*o*-carboranyl)borane. Compound **1** was synthesized *via* salt elimination between monolithiated *o*-carborane and the carborane-based analogue of 9-Br-9-borafluorene. The increase in its Lewis acidity with respect to tris(*o*-carboranyl)borane was confirmed experimentally by Gutmann–Beckett method and computationally through FIA and HIA values. It is noteworthy that unlike the 9-borafluorene system, the exceptional Lewis acidity of **1** primarily stems from the strong inductive effect of *o*-carborane, with negligible (hyper)conjugation effects, as well as the structural constraint imposed by the CC-coupling between two carboranyl groups. These factors combined render it the strongest Lewis acid among triarylboranes, 9-borafluorenes, and their carborane-based analogues. Furthermore, the unique steric environment of **1** allows for its selective addition to the *O*-site of Bestmann ylides, representing a rare example of selective coordination of Bestmann ylides with a borane. Moreover, benefiting from this, a unique reactivity, namely the NHC-catalyzed proton transfer has been disclosed. As demonstrated by this reaction, the combination of selective *O*-complexation and the presence of an acidic proton from the exocyclic carboranyl cage enables the catalytic process.

## Data availability

The data supporting this article have been included as part of the ESI.† Crystallographic data for **1**, **3a**, **3b**, **4a** have been deposited at the Cambridge Crystallographic Data Centre (CCDC) CODE under 2355581–2355583, 2382930 and can be obtained from <https://www.ccdc.cam.ac.uk/structures/>.

## Author contributions

L. X. carried out all the experiments. J. W. performed the DFT calculations. A. M. performed single crystal X-ray diffraction analysis. Q. Y. conceived and supervised the project. All authors discussed the results and contributed to the final manuscript.



## Conflicts of interest

There are no conflicts to declare.

## Acknowledgements

Q. Y. thanks DFG (Grant No. 517941121, 520987585) and Julius-Maximilians-Universität Würzburg (JMU) for financial support. The Center for Computational Science and Engineering at SUSTech is acknowledged for providing computational resources. We thank Christoph Mahler and Liselotte Michels for their help with testing high-resolution mass spectrometry (HRMS) and elemental analysis (EA), respectively.

## Notes and references

- (a) M. Hatano and K. Ishihara, *Lewis Acids*, in *Boron Reagents in Synthesis*, American Chemical Society, 2016, vol. 1236, pp. 27–66; (b) D. S. Matteson, in *Stereodirected Synthesis with Organoboranes*, ed. D. S. Matteson, Springer, Berlin, 1995, pp. 1–20; (c) I. B. Sivaev and V. I. Bregadze, *Coord. Chem. Rev.*, 2014, **270**–271, 75–88; (d) S. M. Berger, M. Ferger and T. B. Marder, *Chem. - Eur. J.*, 2021, **27**, 7043–7058; (e) J. L. Carden, A. Dasgupta and R. L. Melen, *Chem. Soc. Rev.*, 2020, **49**, 1706–1725; (f) A. G. Massey and A. J. Park, *Organomet. Chem.*, 1964, **2**, 245–250; (g) L. Ji, S. Griesbeck and T. B. Marder, *Chem. Sci.*, 2017, **8**, 846–863.
- (a) K. C. Song, K. M. Lee, N. V. Nghia, W. Y. Sung, Y. Do and M. H. Lee, *Organometallics*, 2013, **32**, 817–823; (b) G. Turkoglu, M. E. Cinar and T. Ozturk, *Eur. J. Org. Chem.*, 2017, 4552–4561; (c) H. R. Bhat, P. S. S. Gupta, S. Biswal and M. K. Rana, *ACS Omega*, 2019, **4**, 4505–4518; (d) S. M. Berger and T. B. Marder, *Mater. Horiz.*, 2022, **9**, 112–120; (e) H. Zhao, L. A. Leamera and F. P. Gabbaï, *Dalton Trans.*, 2013, **42**, 8164–8178; (f) K. Ishihara and H. Yamamoto, *Eur. J. Org. Chem.*, 1999, 527–538; (g) A. Chardon, A. D. Mahaut, A. B. Saida and G. Berionni, *Synlett*, 2020, **31**(17), 1639–1648.
- (a) Z. M. Hudson and S. Wang, *Dalton Trans.*, 2011, **40**, 7805–7816; (b) Y. Yu, C. Dong, A. F. Alahmadi, B. Meng, J. Liu, F. Jäkle and L. Wang, *J. Mater. Chem. C*, 2019, **7**, 7427–7432; (c) Z. M. Hudson and S. Wang, *Acc. Chem. Res.*, 2009, **42**(10), 1584–1596; (d) S. Mukherjee and P. Thilagar, *J. Mater. Chem. C*, 2016, **4**, 2647–2662.
- (a) Y. Su and R. Kinj, *Chem. Soc. Rev.*, 2019, **48**, 3613–3659; (b) M. Pramanik and R. L. Melen, *Synthesis*, 2023, **55**, 3906–3918; (c) M. Ghar, M. G. H. Mondal, R. Pal and P. K. Chattaraj, *J. Phys. Chem. A*, 2023, **127**, 4561–4582; (d) D. W. Stephan and G. Erker, *Angew. Chem., Int. Ed.*, 2015, **54**, 6400–6441; (e) N. Zwettler and N. C. Mösch-Zanetti, *Chem. - Eur. J.*, 2019, **25**, 6064–6076.
- (a) J. L. Carden, A. Dasgupta and R. L. Melen, *Chem. Soc. Rev.*, 2020, **49**, 1706–1725; (b) J. P. McInnis, M. Delferro and T. J. Marks, *Acc. Chem. Res.*, 2014, **47**, 2545–2557; (c) E. Y. Chen and T. J. Marks, *Chem. Rev.*, 2000, **100**, 1391–1434; (d) W. E. Piers and T. Chivers, *Chem. Soc. Rev.*, 1997, **26**, 345–354; (e) D. W. Stephan, *Acc. Chem. Res.*, 2015, **48**, 306–316.
- (a) A. Y. Houghton, V. A. Karttunen, W. E. Piers and H. M. Tuononen, *Chem. Commun.*, 2014, **50**, 1295–1298; (b) P. A. Chase, W. E. Piers and B. O. Patrick, *J. Am. Chem. Soc.*, 2000, **122**, 12911–12912; (c) C. Fan, W. E. Piers and M. Parvez, *Angew. Chem., Int. Ed.*, 2009, **48**, 2955–2958; (d) X. Su, T. A. Bartholome, J. R. Tidwell, A. Pujol, S. Yruegas, J. J. Martinez and C. D. Martin, *Chem. Rev.*, 2021, **121**, 4147–4192.
- (a) H. Braunschweig, I. Krummenacher and J. Wahler, *Adv. Organomet. Chem.*, 2013, **61**, 1–53; (b) J. H. Barnard, S. Yruegas, K. Huang and C. D. Martin, *Chem. Commun.*, 2016, **52**, 9985–9991; (c) G. Varvounis, *Comprehensive Heterocyclic Chemistry II*, 1996, vol. 2, pp. 919–932; (d) C. Hong, J. Baltazar and J. D. Tovar, *Eur. J. Org. Chem.*, 2022, e202101343; (e) I. B. Sivaev and V. I. Bregadze, *Coord. Chem. Rev.*, 2014, **270**, 75–88.
- (a) M. Yamashita, *Angew. Chem., Int. Ed.*, 2010, **49**, 2474–2475; (b) J. He, F. Rauch, M. Finze and T. B. Marder, *Chem. Sci.*, 2021, **12**, 128–147; (c) K. Huynh, J. Vignolle and T. D. Tilley, *Angew. Chem., Int. Ed.*, 2009, **48**, 2835–2837; (d) W. Yang, K. E. Krantz, L. A. Freeman, D. A. Dickie, A. Molino, G. Frenking, S. Pan, D. J. D. Wilson and R. J. Gilliard Jr, *Angew. Chem., Int. Ed.*, 2020, **59**, 3850–3852.
- All FIA values are obtained from the same level of calculations: (a) L. Greb, *Chem. - Eur. J.*, 2018, **24**, 17881–17896; (b) M. O. Keeffe, *J. Am. Chem. Soc.*, 1986, **108**, 4341–4344; (c) C. R. Wade, A. E. Broomsgrove, S. Aldridge and P. F. Gabbai, *Chem. Rev.*, 2010, **110**, 3958–3984; (d) L. O. Müller, D. Himmel, J. Stauffer, G. Steinfeld, J. Slattery, G. Santiso-Quiñones, V. Brecht and I. Krossing, *Angew. Chem., Int. Ed.*, 2008, **47**, 7659–7663.
- (a) V. I. Bregadze, *Chem. Rev.*, 1992, **92**, 209–223; (b) M. Scholz and E. H. Hawkins, *Chem. Rev.*, 2011, **111**, 7035–7062; (c) D. Zhao and Z. Xie, *Coord. Chem. Rev.*, 2016, **314**, 14–33; (d) Q. Zao and Z. Xie, *Acc. Chem. Res.*, 2021, **54**, 4065–4079; (e) J. Wang and Q. Ye, *Chem. - Eur. J.*, 2023, **30**, e202303695; (f) J. Wang, L. Xiang, X. Liu, A. Matler, Z. Lin and Q. Ye, *Chem. Sci.*, 2024, **15**, 4839–4845; (g) H. Zhang, J. Wang, W. Yang, L. Xiang, W. Sun, W. Ming, Y. Li, Z. Lin and Q. Ye, *J. Am. Chem. Soc.*, 2020, **142**, 17243–17249; (h) J. Wang, P. Jia, W. Sun, Y. Wei, Z. Lin and Q. Ye, *Inorg. Chem.*, 2022, **61**, 8879–8886.
- (a) Y. Wei, J. Wang, Y. Li, Z. Lin and Q. Ye, *Chem. - Eur. J.*, 2023, **29**, e202203265; (b) C. Zhang, X. Liu, J. Wang and Q. Ye, *Angew. Chem., Int. Ed.*, 2022, **61**, e202205506; (c) C. Zhang, J. Wang, W. Su, Z. Lin and Q. Ye, *J. Am. Chem. Soc.*, 2021, **143**, 8552–8558; (d) C. Zhang, J. Wang, Z. Lin and Q. Ye, *Inorg. Chem.*, 2022, **61**, 18275–18284; (e) M. Diab, K. Jaiswal, D. Bawari and R. Dobrovetsky, *Isr. J. Chem.*, 2023, e202300010; (f) M. O. Akram, J. R. Tidwell, J. L. Dutton and C. D. Martin, *Angew. Chem., Int. Ed.*, 2023, **62**, e202307040; (g) M. O. Akram, C. D. Martin and J. L. Dutton, *Inorg. Chem.*, 2023, **62**, 13495–13504.
- (a) D. Tu, P. Leong, S. Guo, H. Yan, C. Lu and Q. Zhao, *Angew. Chem., Int. Ed.*, 2017, **56**, 11370–11374; (b) J. Li, J. Xu, L. Yan,



- C. Lu and H. Yan, *Dalton Trans.*, 2021, **50**, 8029–8035; (c) M. Chen, J. Xu, D. Zhao, F. Sun, S. Tian, D. Tu, C. Lu and H. Yan, *Angew. Chem., Int. Ed.*, 2022, e202205672.
- 13 (a) Y. Liu, W. Dong, Z. Li and H. Wang, *Chem*, 2021, **7**, 1843–1851; (b) Y. Liu, B. Su, W. Dong, Z. Li and H. Wang, *J. Am. Chem. Soc.*, 2019, **141**, 8358–8363; (c) Y. Xu, Y. Yang, Y. Liu, Z. Li and H. Wang, *Nat. Catal.*, 2023, **6**, 16–22; (d) K. Vashisth, S. Dutta, M. O. Akrama and C. D. Martin, *Dalton Trans.*, 2023, **52**, 9639–9645.
- 14 L. Xiang, J. Wang, I. Krummenacher, K. Radacki, H. Braunschweig, Z. Lin and Q. Ye, *Chem.–Eur. J.*, 2023, **29**, e202301270.
- 15 M. O. Akram, J. R. Tidwell, J. L. Dutton and C. D. Martin, *Angew. Chem., Int. Ed.*, 2022, **61**, e202212073.
- 16 (a) R. Tonner and G. Frenking, *Chem.–Eur. J.*, 2008, **14**, 3260–3272; (b) R. Tonner and G. Frenking, *Chem.–Eur. J.*, 2008, **14**, 3273–3289; (c) L. Zhao, M. Hermann, N. Holzmann and G. Frenking, *Coord. Chem. Rev.*, 2017, **344**, 163–204; (d) H. J. Bestmann and D. Sandmeier, *Chem. Ber.*, 1980, **113**, 274–277.
- 17 (a) U. Mayer, V. Gutmann and W. Gerger, *Monatsh. Chem.*, 1975, **106**, 1235–1257; (b) M. A. Beckett, G. C. Strickland, J. R. Holland and K. A. Sukumar Varma, *Polymer*, 1996, **37**, 4629–4631.
- 18 (a) A. V. Pomogaeva and A. Y. Timoshkin, *ACS Omega*, 2022, **7**, 48493–48505; (b) M. El-Hamdi, M. Sola, J. Poater and A. Y. Timoshkin, *J. Comput. Chem.*, 2016, **37**, 1355–1362; (c) S. B. H. Karnbrock, C. Golz, R. A. Mata and M. Alcarazo, *Angew. Chem., Int. Ed.*, 2022, **61**, e202114550; (d) A. Chardon, A. Osi, D. Mahaut, T.-H. Doan, N. Tumanov, J. Wouters, L. Fusaro, B. Champagne and G. Berionni, *Angew. Chem., Int. Ed.*, 2020, **59**, 12402–12406.
- 19 (a) L. Zapf, M. Riethmann, S. A. Föhrenbacher, M. Finze and U. Radius, *Chem. Sci.*, 2023, **14**, 2275–2288; (b) A. C. Hillier, W. J. Sommer, B. S. Yong, J. L. Petersen, L. Cavallo and S. P. Nolan, *Organometallics*, 2003, **22**, 4322–4326; (c) S. D. González and S. P. Nolan, *Coord. Chem. Rev.*, 2007, **251**, 874–883; (d) M. O. Akram, C. D. Martin and J. L. Dutton, *Inorg. Chem.*, 2023, **62**(33), 13495–13504.
- 20 P. Pérez, L. R. Domingo, A. Aizman and R. Contreras, *Theor. Comput. Chem.*, 2007, **19**, 139–201.
- 21 (a) A. R. Jupp, T. C. Johnstone and D. W. Stephan, *Dalton Trans.*, 2018, **47**, 7029–7035; (b) A. R. Jupp, T. C. Johnstone and D. W. Stephane, *Inorg. Chem.*, 2018, **57**, 14764–14771.
- 22 J. J. Dayl and P. J. Wheatley, *J. Chem. Soc. A*, 1966, 1703–1706.
- 23 (a) M. Alcarazo, C. W. Lehmann, A. Anoop, W. Thiel and A. Fuerstner, *Nat. Chem.*, 2009, **1**, 295–301; (b) R. Bertani, M. Casarin and L. Pandolfo, *Coord. Chem. Rev.*, 2003, **236**, 15–33; (c) L. Pandolfo, G. Paiaro, L. K. Dragani, C. Maccato, R. Bertani, G. Facchin, L. Zanotto, P. Ganis and G. Valle, *Organometallics*, 1996, **15**, 3250–3252.
- 24 A. Brar, D. K. Unruh, A. J. Aquino and C. Krempner, *Chem. Commun.*, 2019, **55**, 3513–3516.
- 25 (a) G. Frenking, R. Tonner, S. Klein, N. Takagi, T. Shimizu, A. Krapp, K. K. Pandey and P. Parameswaran, *Chem. Soc. Rev.*, 2014, **43**, 5106–5139; (b) W. Petz, *Coord. Chem. Rev.*, 2015, **291**, 1–27; (c) A. L. Liberman-Martin, *Cell Rep. Phys. Sci.*, 2023, **4**, 101519.

